





Article

A New Modified Blade Element Momentum Method for Calculating the Aerodynamic Performance of a Wind Turbine in Yaw

Jiaying Wu ¹, Zhenye Sun ¹ , Weijun Zhu ¹ , Shifeng Fu ¹ , Chang Xu ² and Wenzhong Shen ^{1,2,*} 

¹ College of Electrical Energy and Power Engineering, Yangzhou University, Yangzhou 225127, China; mx120220658@stu.yzu.edu.cn (J.W.); zhenye_sun@yzu.edu.cn (Z.S.); wjzhu@yzu.edu.cn (W.Z.); 007452@yzu.edu.cn (S.F.)

² College of Renewable Energy, Hohai University, Chang Zhou 213200, China; zhweifengxu@hhu.edu.cn

* Correspondence: wzsh@yzu.edu.cn

Abstract: The yaw state constitutes a typical operating condition for wind turbines. However, the widely used Blade Element Moment (BEM) theory, due to its adoption of planar disc assumptions, introduces certain computational inaccuracies in yaw conditions. This research aims to develop a new modified BEM method by replacing the momentum theory in traditional BEM with the Madsen analytical linear two-dimensional actuator disc model in order to enhance the accuracy in calculating the aerodynamic performance of yawed wind turbines. Two approaches are introduced to determine the variable parameters in the new modified model: one based on traditional BEM predictions in non-yaw conditions and the other using empirical values determined using experimental data. The new modified model is evaluated against experimental data, CENER FAST, and HAWC2 for the MEXICO rotor. From the comparisons, the new modified method demonstrates closer agreements with experimental values, particularly in the mid and outer parts of the blades. At a wind speed of 15 m/s and a yaw angle of 30°, the discrepancies between computation and measurement are reduced by at least 2.33, 1.22, and 3.25 times at spanwise locations of 60%Radius (R), 82% R , and 92% R , respectively, compared to CENER FAST or HAWC2, demonstrating the feasibility of the proposed methodology.

Keywords: wind turbine; yawed condition; blade element momentum theory; MEXICO rotor



Received: 9 January 2025

Revised: 13 February 2025

Accepted: 19 February 2025

Published: 21 February 2025

Citation: Wu, J.; Sun, Z.; Zhu, W.; Fu, S.; Xu, C.; Shen, W. A New Modified Blade Element Momentum Method for Calculating the Aerodynamic Performance of a Wind Turbine in Yaw. *Energies* **2025**, *18*, 1063. <https://doi.org/10.3390/en18051063>

Copyright: © 2025 by the authors. Licensee MDPI, Basel, Switzerland. This article is an open access article distributed under the terms and conditions of the Creative Commons Attribution (CC BY) license (<https://creativecommons.org/licenses/by/4.0/>).

1. Introduction

The continuous and variable atmospheric wind makes it difficult to promptly track the wind direction, causing the rotational axis of a wind turbine to often not align with the wind direction, which results in the turbine operating under yawed conditions in most cases [1]. In view of this, accurately calculating the load distribution of wind turbines under yawed conditions holds significant academic and practical importance. Actually, the research on wind turbines in yaw is still one of the major design challenges of wind turbines [2,3].

Experimental investigations into the aerodynamic performance of wind turbines under yawed conditions are predominantly conducted through wind tunnel tests. In 2006, various research institutions conducted the MEXICO (Model Experiments in Controlled Conditions) experiments [4–6] for a three-bladed wind turbine in the DNW (German-Netherlands) wind tunnel, where the blade pressure distributions at five radial positions, near-wake flow field, and wake vortex trajectories of the wind turbine under various

operating conditions (including yaw conditions) were obtained. These data can be utilized to validate design methodologies and validate the accuracy of computational methods. Besides, Ozbay [7] conducted experimental tests to measure the power and aerodynamic loads of a scaled-down ERS-100 wind turbine with a rotor diameter of 0.382 m under yawed conditions. Moreover, the National Renewable Energy Laboratory (NREL) in the United States conducted experiments on the Phase VI 19.8 kW small-scale wind turbine, yielding extensive and comprehensive experimental data and the key findings encompassed typical sectional angles of attack under yaw conditions, along with the variation curves of normal aerodynamic loads, tangential aerodynamic loads, and torsional moments as they relate to azimuth angles.

In numerical computations, a few techniques for evaluating the aerodynamic performance of wind turbines under yawed conditions have been developed by several researchers. With the development of computer technology, computational fluid dynamics (CFD) methods have increasingly been employed in the research on the aerodynamic characteristics of wind turbines in yaw. Dong et al. [8] conducted an in-depth analysis and investigation of the aerodynamic performance and load characteristics under various yaw conditions of the NREL 5MW wind turbine model using a CFD-CSD fluid-structure interaction method. Qian et al. [9], based on the MEXICO rotor experiment, studied the aerodynamic performance of wind turbines under yaw conditions by using a CFD method and calculated by RANS (Reynolds-Averaged Navier-Stokes) and DES (Detached Eddy Simulation) models. Although using CFD methods for calculation yields accurate results, substantial computational resources are necessitated, and a relatively prolonged calculation time is entailed. Sørensen and Shen [10], leveraging principles of fluid dynamics, introduced the actuator line model (ALM), which replaces wind turbine blades with virtual rotating lines subjected to volumetric forces. By solving the Navier-Stokes (N-S) equations, the forces on each blade element are calculated and then synthesized to efficiently and accurately compute the loads on the wind turbines under yawed conditions. This approach circumvents the need for a detailed boundary layer resolution in traditional CFD methods, thereby significantly reducing the number of computational grids and the computational time required. Alberto et al. [11] validated the accuracy of the mid-fidelity numerical solver DUST in calculating the aerodynamic performance of wind turbines, including yawed conditions, by analyzing the benchmark NREL-5 MW and Phase VI wind turbines, and some appreciable discrepancies are found as compared to CFD, particularly for the tangential component in yawed conditions.

The Blade Element Momentum (BEM) theory [12–16] is the most efficient and low-cost method to calculate the aerodynamics of wind turbines. However, the accuracy of BEM in calculating aerodynamic forces on wind turbines under yawed conditions is constrained by its assumptions [17–19], such as the planar disc hypothesis and the quasi-steady-state flow hypothesis. Liew et al. [20] proposed a unified momentum model by integrating the BEM with the Generalized Dynamic Wake Theory, offering novel insights into the aerodynamic modeling of wind turbines. Garrel [21] developed an aerodynamic simulation model for wind turbines, named ECN AWSM, based on the principles of nonlinear lift-line vortex wake theory, which serves to mitigate the uncertainties inherent in the currently utilized BEM method. The National Renewable Energy Laboratory (NREL) [22] developed an aeroelastic simulation tool designed to model the dynamic behaviors of horizontal axis wind turbines, integrated with the aerodynamic code AeroDyn. The Technical University of Denmark [23] introduced HAWC2 (version 3.1), a wind turbine response simulation software grounded in multibody formalism that builds upon the classical BEM theory, expanding it to accommodate various aerodynamic effects and enabling simulations of yaw aerodynamic conditions in wind turbines. Moriarty et al. [24] developed an aeroelastic

simulation program tailored for horizontal-axis wind turbines, grounded in a multitude of theories, including the BEM and the Generalized Dynamic Wake Theory, which is capable of predicting the aerodynamic characteristics of wind turbines under various operating conditions, encompassing yaw states among others. However, when using models for calculation, several assumptions are commonly employed, such as the assumption of a planar disc, resulting in that when dealing with aerodynamic parameters under yaw conditions of wind turbines, the accuracy of these calculations may be compromised, and few numerical models have been developed specifically for yaw conditions at present.

The present research deals with the development of a new modified computational methodology aiming at accurately determining the aerodynamic forces on wind turbines under yawed conditions. Specifically, the Madsen analytical linear two-dimensional actuator disc model [25] and the Blade Element Theory are combined in this paper to calculate the aerodynamic forces on wind turbines under both non-yawed and yawed conditions. During the validation of the model, a comparative analysis was conducted between the data obtained at a 0° yaw angle and the computational results derived from the traditional BEM theory, revealing the existence of discrepancies, as a result of which this paper aims to introduce a new parameter into the Madsen analytical linear two-dimensional actuator disc model and, through a comparative analysis with the traditional BEM theory, accurately delineating the variable parameter within the new modified model and the parameter is then applied to compute the aerodynamic loads on wind turbine blades under yawed scenarios.

The paper is organized as follows: Section 2 presents the BEM theory developed in this paper and the calculation steps to use the new modified method. Calculation results and comparisons of the new modified method with other methods and the limitations of the new modified model are given in Section 3. Finally, conclusions are drawn in Section 4.

2. Numerical Methods

This section primarily presents the new modified BEM method to calculate the aerodynamic performance of wind turbines in yaw states. The new modified BEM consists of the Blade Element theory and the Madsen analytical linear two-dimensional actuator disc model (Madsen model) [25] that are pertinent to the yaw phenomena. Finally, the calculation procedure of the new modified model is provided.

2.1. New Modified Blade Element Momentum Theory

The new modified Blade Element Momentum (BEM) method, consisting of the Madsen model and the blade element theory, allows for the obtaining of induction factors, encompassing the axial induction factor a and the tangential induction factor a' , thereby facilitating the computation of the aerodynamic forces on a wind turbine. Distinguishing from the classical BEM approach, the present study adopts the Shen tip correction [26–28] and the Spera correction [29].

The Blade Element Theory is an analytical approach that divides a blade of a wind turbine into multiple independent units, known as blade elements, along its spanwise direction. Given that Blade Element Theory is a classical theory, this paper solely elucidates the modifications to the yaw component and the associated formulas within the traditional Blade Element Theory.

For a blade element located at a radial distance r from the blade root, under conditions of an inflow wind speed V_o , a rotational angular velocity ω , a yaw angle γ , the axial velocity V_n , tangential velocity V_t , and relative resultant velocity V_{rel} are, respectively, given by the following:

$$V_n = V_o(\cos \gamma + W_n / V_o) \quad (1)$$

$$V_t = V_0(-\sin \gamma \cos \Psi + W_t/V_0) + \omega r \quad (2)$$

$$V_{rel} = \sqrt{V_n^2 + V_t^2} \quad (3)$$

where, W_n and W_t represent the axial induced velocity and the tangential induced velocity, respectively, which can be derived through the integration with a momentum theory, Ψ represents the azimuthal angle of a blade as it rotates clockwise, with 0 degree indicating the blade pointing upwards. The inflow angle φ is formed between the relative resultant velocity and the plane of rotation and can be calculated by $\varphi = \tan^{-1} \frac{V_n}{V_t}$. From this, the angle of attack α for the blade element can be derived by $\alpha = \varphi - \theta$, where θ represents the local pitch angle, being the local angle between the chord line and the plane of rotor rotation. It is a combination of the pitch angle θ_p and the blade twist angle β , numerically equivalent to the sum of these two angles. By utilizing the angle of attack α , one can obtain the corresponding lift coefficient C_l and drag coefficient C_d through a consultation of an airfoil parameter table. On this basis, with the air density ρ , the number of blade B , for an airfoil with a chord length of c , the thrust δT generated along a section of an airfoil with a spanwise length of δr can be calculated using the following equations:

$$dT = \frac{1}{2} \rho V_{rel}^2 B c (C_l \cos \varphi + C_d \sin \varphi) dr F_1 \quad (4)$$

where F_1 is the tip loss factor developed by Shen et al. [26–28]:

$$\begin{cases} F_1 = \frac{2}{\pi} \cos^{-1} \left[\exp \left(-g \frac{B(R-r)}{2R \sin \varphi} \right) \right] \\ g = \exp[-0.125(B\lambda - 21)] + 0.1 \end{cases} \quad (5)$$

In Equation (5), R is the radius of rotor, and the tip speed ratio λ is defined by $\lambda = \frac{\omega R}{V_0}$. By integrating Equation (4), the overall thrust (T) of the wind turbine can be obtained, and from this, the thrust coefficient C_{T_m} can be calculated by the following:

$$C_{T_m} = \frac{T}{\frac{1}{2} \rho V_0^2 \pi R^2} \quad (6)$$

The traditional momentum theory employs the planar disc hypothesis, which gives rise to heightened errors in the computations undertaken by the BEM. For this reason, the Madsen analytical linear two-dimensional actuator disc model, a model formulated as an integral 1-dimensional (1-D) momentum theory to delve more deeply into the flow characteristics of the actuator disk (AD) and then developed an analytical solution to a yawed disc with constant loading by a simple coordinate rotation, is used in this study. Its core concept is treating the wind turbine rotor as an infinitely thin disc through which forces are imparted to the fluid, thereby enabling the calculation of the aerodynamic behaviors of the yawed wind turbine. The primary objective of this model is to offer a simplified yet unified computational approach for accurately assessing the induction effects of wind turbine rotors, particularly under complex flow conditions such as yaw and cone. This section will outline the core content of the model employed in the present study.

The primary application of the Madsen analytical linear two-dimensional actuator disc model is to compute the induction factors under yaw conditions.

Within this research, a comprehensive coordinate system has been constructed, with its origin placed at the epicenter of the wind turbine's rotating plane, and in this system, the x' -axis is meticulously defined as being perpendicular to the very plane of the wind turbine, while concurrently ensuring that the y' -axis is orthogonal to the x' -axis, thereby establishing a robust framework in which the horizontal and vertical coordinates of the

observation point are respectively denoted by x' and y' . Its core computational formula articulated as follows:

$$W_x = \frac{\Delta p}{2\pi} \left(\tan^{-1} \frac{1-y'}{x'} + \tan^{-1} \frac{1+y'}{x'} \right) - \Delta p \quad (7)$$

$$W_y = \frac{\Delta p}{4\pi} \ln \frac{x'^2 + (y'+1)^2}{x'^2 + (y'-1)^2} \quad (8)$$

$$W_{n1} = W_x \cos \gamma - W_y \sin \gamma \quad (9)$$

However, during the validation process of the model, this paper conducted a comparative analysis using data from a 0-degree yaw angle against the calculations based on a traditional BEM theory and identified the discrepancies. In light of this, the present study introduces an adjustable factor m to modify Equation (7), thereby altering the calculation of the axial induction factor and significantly enhancing the accuracy of the model. The introduction of m is an empirical correction, and the methods for its determination will be introduced in Section 2.2.

$$W_x = \frac{\Delta p}{2\pi} \left(\tan^{-1} \frac{1-y'}{x'} + \tan^{-1} \frac{1+y'}{x'} \right) - m\Delta p \quad (10)$$

The axial induction velocity W_n and the induction factor a in the yaw state can be calculated by the following:

$$W_n = W_{n1} V_o \quad (11)$$

$$a = -\frac{W_n}{V_o \cos \gamma} \quad (12)$$

For a yawed wind turbine, it needs to calculate the induced velocity at the rotor, therefore set $x' = 0, y' = \frac{r \sin \Psi}{R} \cos \gamma - x' \sin \gamma$. Moreover, the $W_x, W_y,$ and W_{n1} are the induced velocities after the dimensionless treatment of the flow velocity V_o , while Δp represents the pressure difference non-dimensionalized by ρV^2 and it can be calculated by the following equation:

$$\begin{cases} C_{Tl} = C_{Tm} \frac{2}{1 + \sqrt{1 - C_{Tm}}} \\ \Delta p = \frac{1}{2} C_{Tl} \end{cases} \quad (13)$$

where, C_{Tm} is the thrust coefficient of the wind turbine which can be calculated by Equation (6).

Moreover, the model can be utilized as a rotor induction model with the prerequisite of being integrated with an angular momentum model for the tangential induction velocity W_t . This integration can be achieved by adopting the modeling approach outlined by Madsen et al. [30], using the equation derived from the balance of angular momentum across the actuator disc, in conjunction with a blade element analysis.

$$W_t = \frac{V_o C_Q}{2(1-a)} \quad (14)$$

and C_Q is the non-dimensional tangential load coefficient defined as the following:

$$C_Q = \frac{V_{rel}^2 B c (C_l \sin \varphi - C_d \cos \varphi) F_1}{V_o^2 2\pi r} \quad (15)$$

where F_1 is the Shen tip loss function, and the other variables are mentioned above. The tangential induced velocity a' can be derived from $a' = \frac{W_t}{V_o \cos \gamma}$.

2.2. Numerical Procedure

The present study aims to develop a new modified method that integrates the Blade Element Theory with the Madsen analytical linear two-dimensional actuator disc model, to achieve more accurate assessments of the aerodynamic loads experienced by wind turbines under yawed conditions.

The core components of the model are introduced as follows:

Step 1: Determine the geometric parameters of a wind turbine in consideration, encompassing chord lengths c , twist angles β , and selected airfoil profiles at various positions along the blades. Additionally, the key environmental conditions in which the wind turbine operates also must be specified, including the incoming wind speed V_o , yaw angle γ , and air density ρ .

Step 2: Set initial values for the induced velocities W_n , W_t , and thrust T . In this paper, we establish the initial conditions as follows: $W_n = 0$, $W_t = 0$. Given that the thrust coefficient of a wind turbine exhibits a value of 0.89 when its power coefficient reaches its peak, the initial value for the thrust coefficient C_{T_m} was therefore set to 0.89 ($C_{T_m} = 0.89$) in the present study, and then the initial value of total thrust T can be calculated by $T = \frac{1}{2}\rho V_o^2 \pi R^2 C_{T_m}$.

Step 3: The thrust coefficient C_{T_m} is derived using the thrust T , and the value of Δp is calculated according to Equation (13).

Starting from Step 4 to Step 8, the calculations are conducted for each azimuthal angle and each blade cross-section.

Step 4: Calculate the local axial velocity V_n , local tangential velocity V_t , local resultant inflow velocity V_{rel} , and inflow angle φ by computing the arctangent of the ratio of V_n to V_t , from which the angle of attack α is obtained.

Step 5: Use the angle of attack α to retrieve the corresponding lift coefficient C_l and drag coefficient C_d from a lift-drag coefficient table or curve.

Step 6: Calculate the tip correction factors F_1 to correct for errors arising from tip loss effects.

Step 7: Calculate the new values of the local axis velocity W_n using Equations (8)–(11).

The tangential induced velocity can be calculated by using Equations (14) and (15). In order to enhance the convergence, a relaxation factor χ is used in the calculation of W_n and W_t .

$$\begin{cases} W_{nk} = \chi W_{nk} + (1 - \chi) W_{nk-1} \\ W_{tk} = \chi W_{tk} + (1 - \chi) W_{tk-1} \end{cases} \quad (16)$$

Step 8: Based on the W_n and W_t values obtained in Step 7, V_{rel} is corrected, and subsequently, the axial force $F_n = \frac{1}{2}\rho V_{rel}^2 c (C_l \cos \varphi + C_d \sin \varphi) F_1$, tangential force $F_t = \frac{1}{2}\rho V_{rel}^2 c (C_l \sin \varphi - C_d \cos \varphi) F_1$ at the corresponding azimuthal angle and blade element position of the blade, as well as the thrust of the respective airfoil section dT , are further calculated.

Steps 9 and 10 are to calculate the whole parameters of the wind turbine.

Step 9: Compare W_n and W_t at each azimuthal angle and each blade section obtained in the current iteration with those from the last iteration. If the maximum difference between them is less than a threshold of 10^{-10} , the iteration is deemed to be converged, and the relevant parameters are output; otherwise, the process returns to Step 4 for another round of calculation until the convergence condition is met.

Step 10: Output the power and thrust in function of azimuth angle, among other relevant characteristics.

A flow diagram of the model is shown in Figure 1.

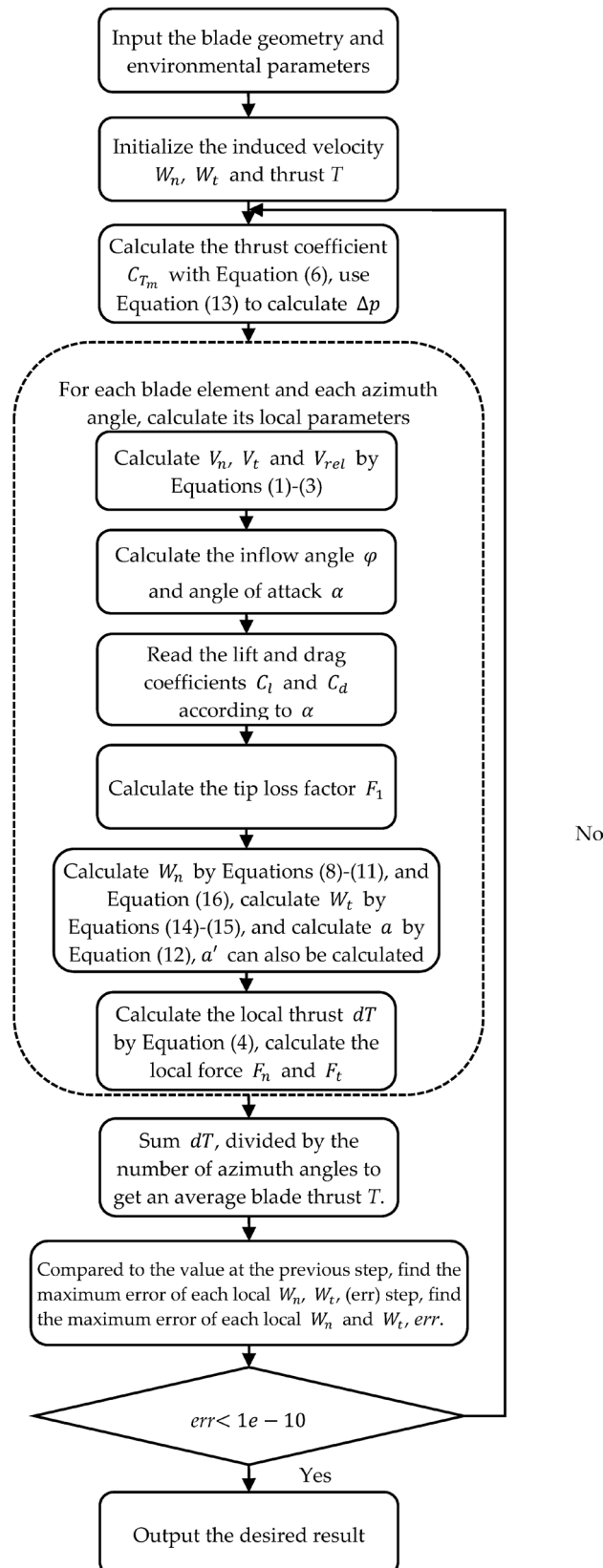


Figure 1. Flowchart for the new modified model.

One of the pivotal elements in applying this model lies in accurately determining the variable parameters m in Equation (10). This paper introduces two distinct methodologies for establishing the value of m .

The first method takes the BEM model in yaw-free conditions. The initial step involves utilizing the traditional BEM to output the axial induction factor a of the target wind turbine under predefined environmental parameters with a yaw angle of 0° . Subsequently, to minimize the difference between the a values calculated by the two models, the *fmincon* function in the MATLAB R2022b optimization toolbox is used to obtain the specific values of the variable parameter m at different radial positions. The *fmincon* function uses an interior point algorithm introduced in Reference [31], and the value of m varies for each operating condition and changes along the blade span in this method. Based on this, while keeping other environmental variables (such as velocity, pitch angle, tower height, and so on) constant, the yaw angle to be calculated is adjusted, and the variable parameter m obtained in the previous step is substituted into the new modified model for recalculation. Through this process, the load distribution of the wind turbine blades at different radial positions and azimuth angles can be obtained under the required yaw angle conditions.

The rationale behind the introduction of the second methodology pertains to the potential variability of the parameter m with respect to the yaw angle. The first approach, which employs a constant value of m equal to that used under non-yaw conditions, may inadvertently amplify the model's predictive errors. In contrast, the second approach employs empirical values of the parameter m , derived from experimental data across various yaw angles, as demonstrated in Table 1. To streamline computational processes, the m solely varies with the yaw angle. The objective is to minimize the average of the differences between the computed and experimental values of the axial and tangential forces acting on the blades at various spanwise positions and azimuthal angles. This is achieved by utilizing the *fmincon* function mentioned above. Given that m is instrumental in the computation of the dimensionless axial induction factor a , these empirically derived values are, in theory, broadly applicable.

Table 1. m values at different yaw angles.

Yaw Angle	m -Value
0°	1.10
15°	1.95
30°	1.30

3. Results and Comparisons

To validate the accuracy of the model and the impact of various yaw angles on a wind turbine, this section benchmarks against the data from the MEXICO (Model Experiments in Controlled Conditions) experiment, which measured a three-bladed wind turbine model with 4.5 m diameter in the $8 \times 6 \text{ m}^2$ open test section of DNW-LLF (German-Dutch Wind Tunnel-Large Low-speed Facility) wind tunnel. The geometric parameters and the comprehensive setup of the experimental parameters of the MEXICO rotor are specified in reference [6], and some key parameters are introduced in Table 2.

Table 2. Key blade geometry and experimental conditions.

	Parameters	Value
Blade geometry	Rotor radius [m]	2.25
	Hub radius [m]	0.21
Experimental conditions	Rotational speed [rpm]	424.5
	Pitch angle [degree]	-2.3

This section compares the computational results of the new modified model with those obtained from the CENER FAST and the HAWC2. The CENER FAST code, as referenced in [22], is an aeroelastic simulation tool capable of modeling the dynamic behavior of horizontal axis wind turbines, coupled to the aerodynamic code AeroDyn, which calculates the lift, drag, and pitching moment coefficients on each section of a blade as well as the forces on each of the elements along the span. The HAWC2 code is formalized on the basis of multibody dynamics and is capable of addressing the constraints associated with complex structures and large-scale rotating mechanisms, as elaborated in detail in reference [19]. The result of them for MEXICO can be seen in reference [6]. Given that reference [6] on yawed conditions is limited to the specific combinations of a wind speed at 15 m/s with a yaw angle of 30° and a wind speed at 24 m/s with a yaw angle of 15°, this paper similarly focuses on these two scenarios when discussing yawed conditions. Moreover, two distinct approaches for the utilization of parameter m are presented; for clarity in our exposition, the term “new modified BEM1” corresponds to the model calculations employing the first method of m , while “new modified BEM2” signifies the computational outcomes based on the second approach of m . Collectively, these two approaches are referred to as the “new modified model”. Furthermore, the implementation of the novel modified methodology necessitates an initial comparison with the BEM under non-yawed conditions to ascertain the variable parameter m , which is subsequently utilized for calculations in yawed scenarios, so the computational results of the new modified model under non-yawed conditions are also presented in this section.

3.1. MEXICO Rotor in Axial Flow Conditions

This section compares the results where the yaw angle is set to 0° at the wind speeds of 10 m/s, 15 m/s, and 24 m/s. Under the non-yawed condition, the force exerted on the blades remains unchanged in the azimuth angle. Consequently, during this case, the emphasis is exclusively on examining the axial and tangential forces that correspond to varying radial distance from the rotor center. r represents the radial distance from the rotor center, and R is the radius of the rotor.

The blade axis forces at the three wind speeds are plotted in Figure 2. In general, when compared to the CENER FAST and HAWC2 models, the new modified model demonstrates a higher degree of accuracy in approximating experimental values, and the results from the new modified BEM1 and new modified BEM2 essentially coincide under wind speeds of 15 m/s and 24 m/s. Furthermore, after the parameter m is fitted using an interior point algorithm, the calculations of the new modified BEM1 under unbiased yaw conditions exhibit near-identical results to those of the BEM model. Specifically, at a wind speed of 10 m/s, the axial forces calculated by the new modified BEM1 are closely aligned with experimental data from root to a radius of 82% spanwise station. However, near the blade tip (at a radius of $0.92R$), the predicted values are much lower than the experimental values. Compared to the calculations from the CENER FAST and the HAWC2, the new modified BEM1 demonstrates overall superior accuracy, except at a radius of $0.92R$; its error margin is slightly larger than that of the CENER FAST code and the new modified BEM2. Under wind speeds of 15 m/s, the computational values of the new modified model are basically consistent with the experimental data. When compared to the computational values obtained from CENER FAST and HAWC2, the results of the new modified model present a smaller error in all measurement positions. At a wind speed of 24 m/s, within the range where the radial ratio is less than $60\%R$, the predictive values of the new modified model are marginally lower than the experimental observations. Conversely, when the radial ratio exceeds $60\%R$, the predictive values of the new modified model surpass the experimental observations. Overall, the discrepancies between the predictive values of

the new modified model and the experimental observations are insignificant, and when compared to the CENER FAST code and the HAWC2 code, the new modified model demonstrates a lower level of error.

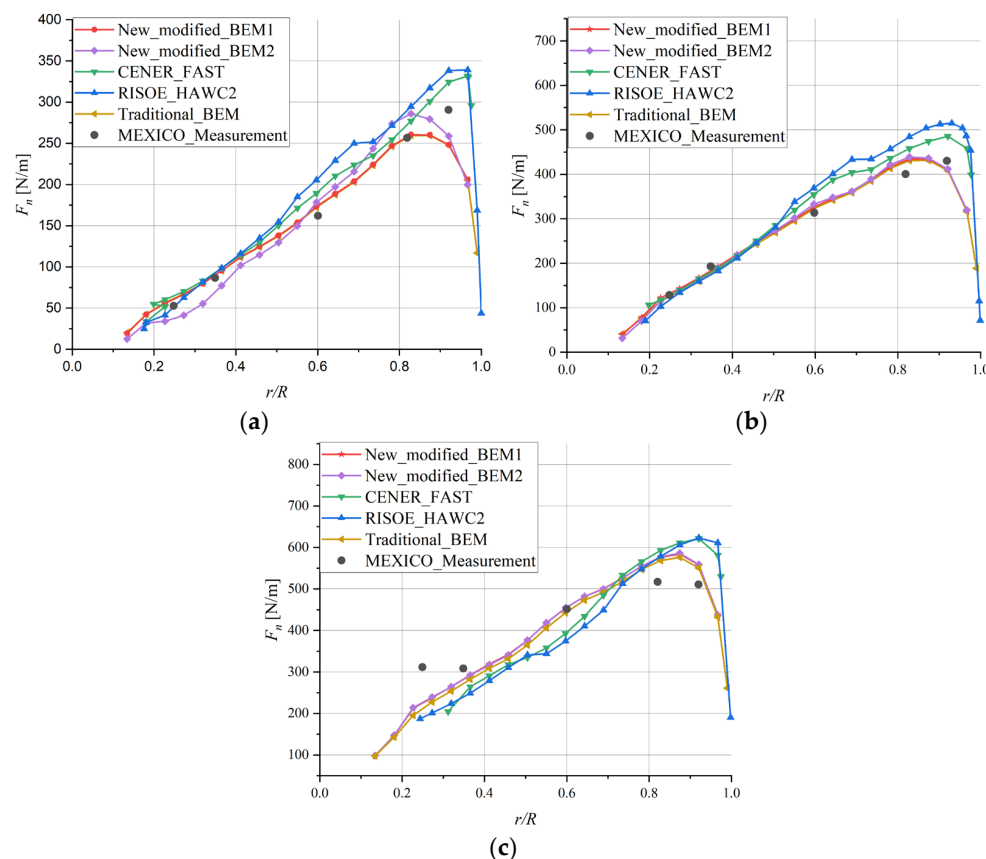


Figure 2. Axial forces on the MEXICO rotor at wind speeds of (a) 10 m/s, (b) 15 m/s, (c) 24 m/s.

The blade tangential forces at the three wind speeds are plotted in Figure 3. Analogous to the axial forces, the computational results obtained from the new modified BEM1, after undergoing m -value adjustment utilizing an interior point algorithm, exhibit a high degree of proximity to those derived from the BEM under non-yaw conditions, and the outcomes derived from the new modified BEM1 and the new modified BEM2 are essentially identical under wind speeds of 15 m/s and 24 m/s. At a wind speed of 10 m/s, as the distance from the blade root increases, the computed values of the new modified model initially slightly underestimate the experimental values before surpassing them. At a wind speed of 15 m/s, the computed values, which have been obtained from the three models, demonstrate a high degree of proximity, and upon comparison with the experimental values, are found to be associated with relatively minor deviations. Under conditions of a wind speed of 24 m/s, when the ratio r is less than $0.6R$, the predicted values of the three models are lower than the experimentally measured values. Conversely, at equal to $0.82R$ and $0.92R$, the predicted values of the models exceed the measured values. It is noteworthy that, except for the case where equals $0.82R$ and the error between the predicted and measured values of the new modified model is slightly higher than that of the HAWC2 code, in all other instances, the prediction errors of the new modified model are lower than those of the other models.

In general, when the variable parameter is adjusted using the interior-point algorithm, the new modified BEM1 yields results that closely approximate those achieved by the traditional BEM in calculating the aerodynamic characteristics of wind turbines under non-yaw conditions, thereby effectively capitalizing on the traditional BEM strength in precisely determining aerodynamic properties under these conditions. The “new modified

BEM2”, which utilizes empirical values, exhibits a slight deviation from the “new modified BEM1” at a wind speed of 10 m/s, although the difference is not significant. At wind speeds of 15 m/s and 24 m/s, the computational results from both methods are essentially superimposed and exhibit minor deviations from experimental data, suggesting that the new modified BEM2 is also capable of accurately predicting the aerodynamic performance of wind turbines at zero yaw angles. Under the condition of a yaw angle of 0° , for both axial and tangential forces, the prediction values of the new modified model exhibit smaller deviations from the experimental data in most cases, in comparison with the CENER FAST and the HAWC2, and this proves that the new modified model can still be used under the condition of no yaw.

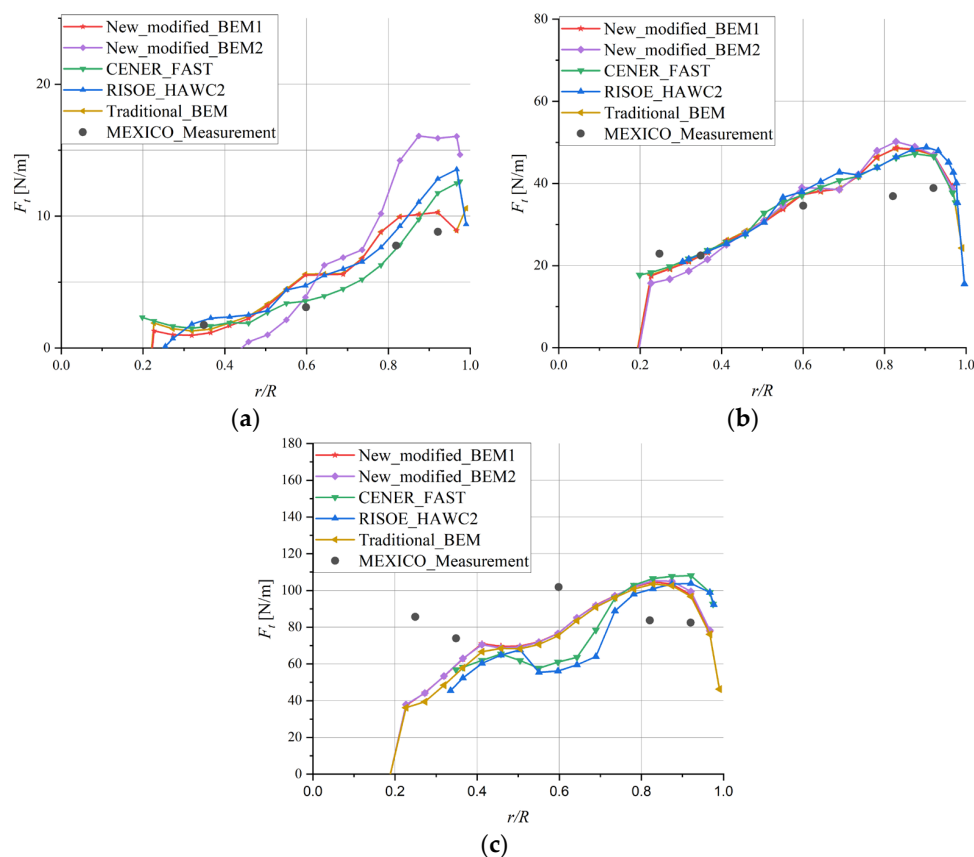


Figure 3. Tangential forces on the MEXICO rotor at wind speeds of (a) 10 m/s, (b) 15 m/s, (c) 24 m/s.

3.2. MEXICO Rotor at a Wind Speed of 15 m/s and a Yaw Angle of 30°

Under yaw conditions, changes in azimuth angle will lead to alterations in the relative position between a blade and the incoming wind, thereby influencing the force experienced on the blade. In light of this, it is necessary to conduct an in-depth investigation into the dynamic characteristics of the tangential and axial forces acting on the blade throughout its complete rotational cycle. For this section, the focus is on studying the force distribution on the blade at different azimuth angles and radial distances from the rotor center when the incoming wind speed is 15 m/s and the yaw angle is set to 30° . Furthermore, it presents a comparative analysis of the relative errors (err) exhibited by different models across various spanwise locations on the blade, thereby contributing to a more nuanced understanding of model prediction accuracy. The calculation method of model relative error in this paper is as follows:

$$err = \frac{\sum_{i=1}^n \frac{abs(F_{model_i} - F_{measure_i})}{F_{measure_i}}}{n} \times 100\% \quad (17)$$

where F_{model_i} is the calculated force of the model corresponding to the i -th azimuth angle, $F_{measure_i}$ is the measurement value of the MEXICO experiment corresponding to the i -th azimuth angle, accordingly. n is the number of azimuth angles. The err is the average relative error of the model for each azimuth of the experimental value, which can represent the accuracy of the model, and the smaller the error, the more accurate the model.

Figure 4 presents the variation of axial force at different spanwise locations of the blade with the azimuthal angle, and Table 3 is the relative error comparison of the three models under the conditions of a wind speed of 15 m/s and a yaw angle of 30 degrees. When the r/R is equal to 0.25 and 0.35, the predictions from the HAWC2 code are greater than the new modified model. This phenomenon can be attributed to the design characteristic of the MEXICO rotor, where the hub diameter exceeds 10% of the overall rotor diameter, thereby significantly influencing the aerodynamic characteristics in the region adjacent to the hub. It is noteworthy that, during the process of constructing the new modified model, the influence of the hub effect was not adequately accounted for, resulting in a direct reduction in the calculation accuracy to below the desired level in the aforementioned two scenarios. Conversely, at r/R values of 0.6, 0.82, and 0.92, which correspond to locations closer to the blade tip, the average errors of the newly proposed model are significantly smaller than those of the CENER FAST and the HAWC2, with the maximum improvement of 7.67 times over traditional models observed at the 92% spanwise position of the blade. Given that the axis force exerted on the blade tip is more pronounced as compared to that on the blade root, and in most instances, the new modified model outperforms the aforementioned two traditional models under this operating condition. In comparison to the new modified BEM1, the new modified BEM2 exhibits enhanced precision at most spanwise blade locations. This indicates that making the variable parameter m to vary with changes in the yaw angle can enhance the predictive accuracy of the model.

Table 3. Comparison of axial force relative errors of three models at a wind speed of 15 m/s and a yaw angle of 30°.

Spanwise Position	New Modified BEM1	New Modified BEM2	HAWC2	CENER FAST
25%	19%	14%	7%	28%
35%	12%	13%	10%	16%
60%	6%	4%	22%	14%
82%	9%	6%	21%	11%
92%	3%	4%	23%	13%

Figure 5 presents the distribution of tangential forces measured at radial positions of 25%, 35%, 60%, 82%, and 92% of the blade span, under conditions of a wind speed of 15 m/s and a yaw angle set at 30 degrees. Due to the small values of tangential force and the incomplete values given in the reference [6] at $r/R = 60\%$, the quantitative comparison of relative error is not done here. At the radial position of 25% of the blade span, the new modified BEM1 demonstrates a higher degree of congruence as compared with HAWC2, with an error range that is comparable to that of CENER FAST, but the new modified BEM2 exhibits a larger discrepancy, which may be attributable to the model's omission of hub effects. At the position $r/R = 0.35$, the predictions of CENER FAST exhibit a higher degree of agreement with the experimental data as compared to the new modified model and HAWC2. This may also be because the new modified model does not take into account hub effects. It is noteworthy that the new modified BEM2 computational results align closely with experimental values during the rotation of the blade through the lower half-circle (where the azimuthal angle ranges between 90° and 270°), which underscores the potential

of the new modified BEM2 in accurately capturing aerodynamic behaviors under specific operational conditions. At the position $r/R = 0.6$, upon comprehensive evaluation, the average error of the new modified BEM1 is 23%, and the new modified BEM2 is 4%, which is much lower than the 32% of CENER FAST and the 31% of HAWC2. At the radial position of 82% and 92%, the amplitude of the calculated results of CENER FAST varies greatly with the azimuth angle, and the calculated values of the new modified model are close to those of the HAWC2, but the calculated results of the new modified model, especially the new modified BEM2, have a higher agreement with the experimental observed values in most cases. In general, the new modified model provides predictions that are relatively close to the experimental data at most spanwise positions and azimuthal angle ranges.

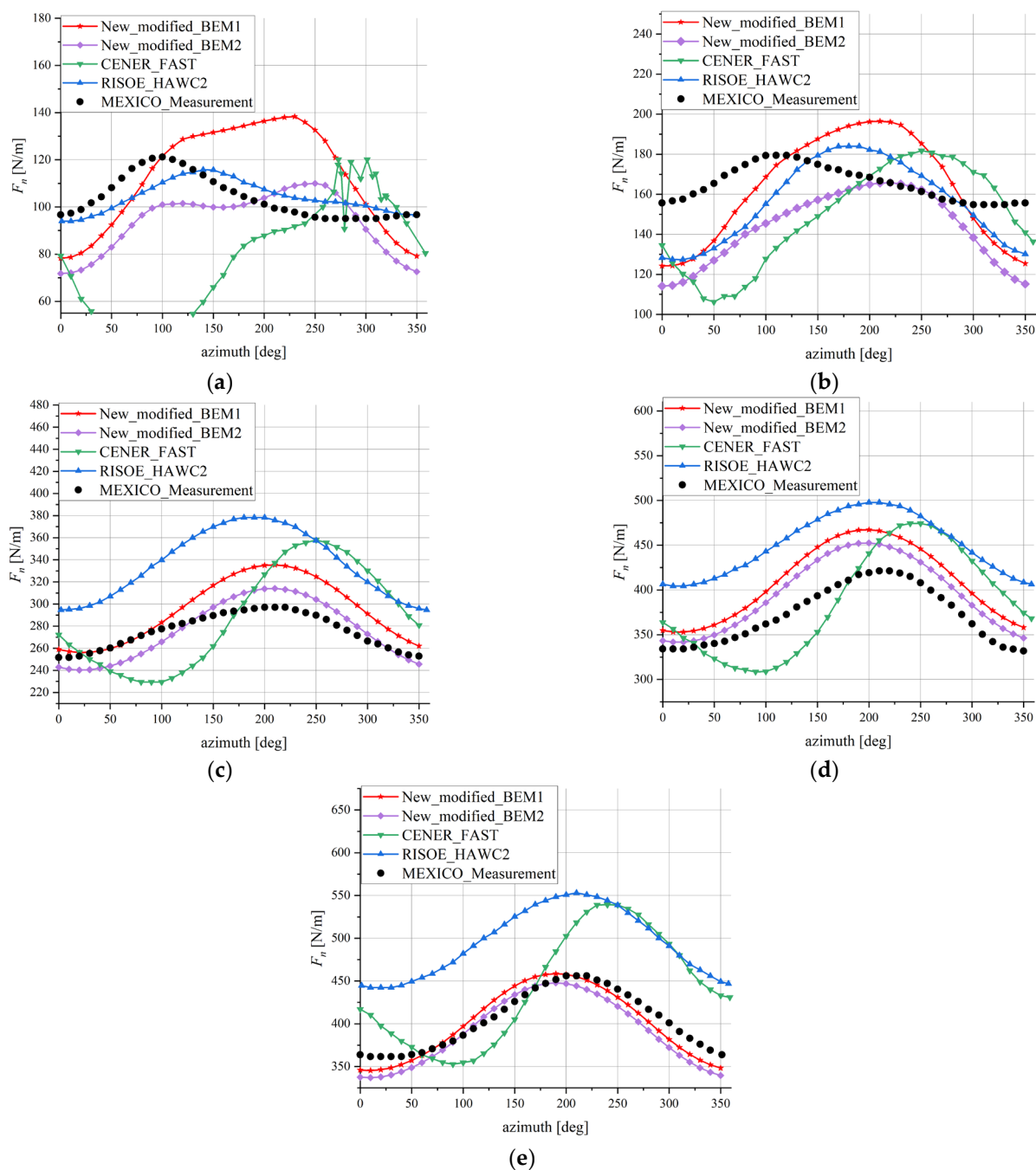


Figure 4. Axial force variation with azimuth angle on the MEXICO rotor at a wind speed of 15 m/s, a yaw angle of 30° and the span station (r/R) of (a) 25%, (b) 35%, (c) 60%, (d) 82%, and (e) 92%.

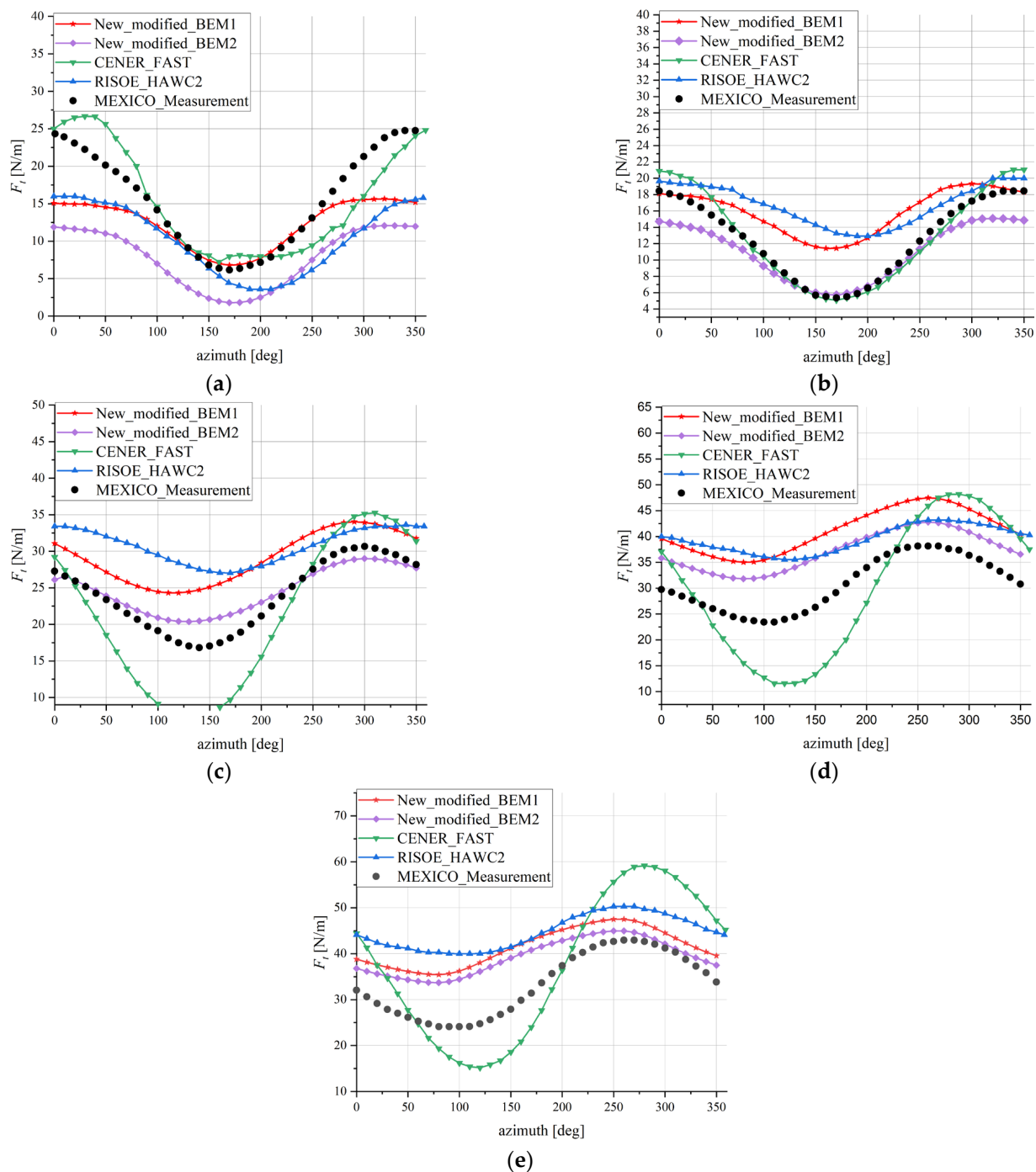


Figure 5. Tangential forces variation with azimuth angle on the MEXICO rotor at a wind speed of 15 m/s, a yaw angle of 30° and the span station (r/R) of (a) 25%, (b) 35%, (c) 60%, (d) 82%, and (e) 92%.

3.3. MEXICO Rotor at a Wind Speed of 24 m/s and a Yaw Angle of 15°

This section is designed to evaluate the predictive accuracy of the model under high wind speed conditions. Specifically, this condition focuses on computing the distribution of axial and tangential forces at various radial positions characterized by the ratio of radial distance to rotor radius (r/R) of 0.25, 0.35, 0.60, 0.82, and 0.92, within an environment where the wind speed is set at 24 m/s and the yaw angle is fixed at 15°.

Figure 6 illustrates the axial force characteristics of the MEXICO rotor as it varies with different azimuth angles, and Table 4 is the relative error comparison of the three models, under the conditions of a yaw angle set at 15° and a constant wind speed of 24 m/s. The

comparison reveals that the new modified BEM1 exhibits lower average prediction errors at all measured radial span positions ($r/R = 0.25, 0.35, 0.6, 0.82, 0.92$) and is significantly lower than those of HAWC2 and CENER FAST. Moreover, in the regions closer to the root ($r/R = 0.25, 0.3$), the errors associated with the new modified BEM1 are less than those of the new modified BEM2, while in the sections farther from the root ($r/R = 0.6, 0.82, 0.92$), the new modified BEM2 demonstrates lower errors than the new modified BEM1. At $r/R = 0.25$, the experimental values of the MEXICO rotor exhibit minimal fluctuation in azimuth angle. It clearly reveals that, compared to the HAWC2 model, the values calculated by the new modified model are closer to the experimentally measured values at all azimuth angles, and the values of CENER FAST align more closely with the experimental data only when the blade rotates to positions near-vertical orientation, with relatively larger errors observed at most other azimuth angles. When $r/R = 0.35$, the new modified BEM1 retains its significant advantage in computational accuracy, with its calculated values at all azimuth angles being closer to the experimental values than those of HAWC2. Although the FAST values are slightly closer to the experimental data within the azimuth angle ranges greater than 240° and less than 20° , its errors remain relatively large across the majority of other azimuth angles, but it should be noted that the accuracy of the new modified BEM2 is comparatively lower than that of HAWC2 in this condition. At $r/R = 0.6$, obviously, the calculated values of the new modified model are very close to the experimental values. The precision of the new modified model is at least 1.4 times higher and up to 4.3 times higher than those of traditional models. For the case of $r/R = 0.82$, although the predictive values of all three models overestimate the experimental values, the predictive value of the new modified model is slightly lower than those of HAWC2 and CENER FAST, thus closer to the experimental data. At the position near the blade tip, where $r/R = 0.92$, since the information of the calculated value of HAWC2 and CENER FAST between 80 degrees and 140 degrees in the literature is blocked by the icon, this paper uses the spline interpolation method [32] to complete the information at this position. The predictive values of all three models are higher than the experimental values. Among them, the predictive values of HAWC2 and CENER FAST are relatively close, while the new modified model, although consistent with them in trend, exhibits significantly smaller values at each azimuth angle, thereby being closer to the experimental values and achieving at least a twofold improvement in accuracy compared to the traditional models. In summary, when predicting the axial force of the MEXICO rotor at different azimuth angles and radial positions, the new modified model demonstrates lower prediction errors compared to HAWC2 and CENER FAST, and in regions away from the hub, the error associated with new modified BEM2 is smaller than that of BEM1 at each azimuth angle. Notably, in the critical regions of the blade, the predictive accuracy of the new modified model is significantly improved, aligning more closely with the experimental observations.

Table 4. Comparison of axial force relative errors of three models at a wind speed of 24 m/s and a yaw angle of 15° .

Spanwise Position	New Modified BEM1	New Modified BEM2	HAWC2	CENER FAST
25%	26%	38%	37%	47%
35%	11%	22%	27%	14%
60%	5%	3%	13%	7%
82%	18%	12%	20%	23%
92%	13%	10%	26%	29%

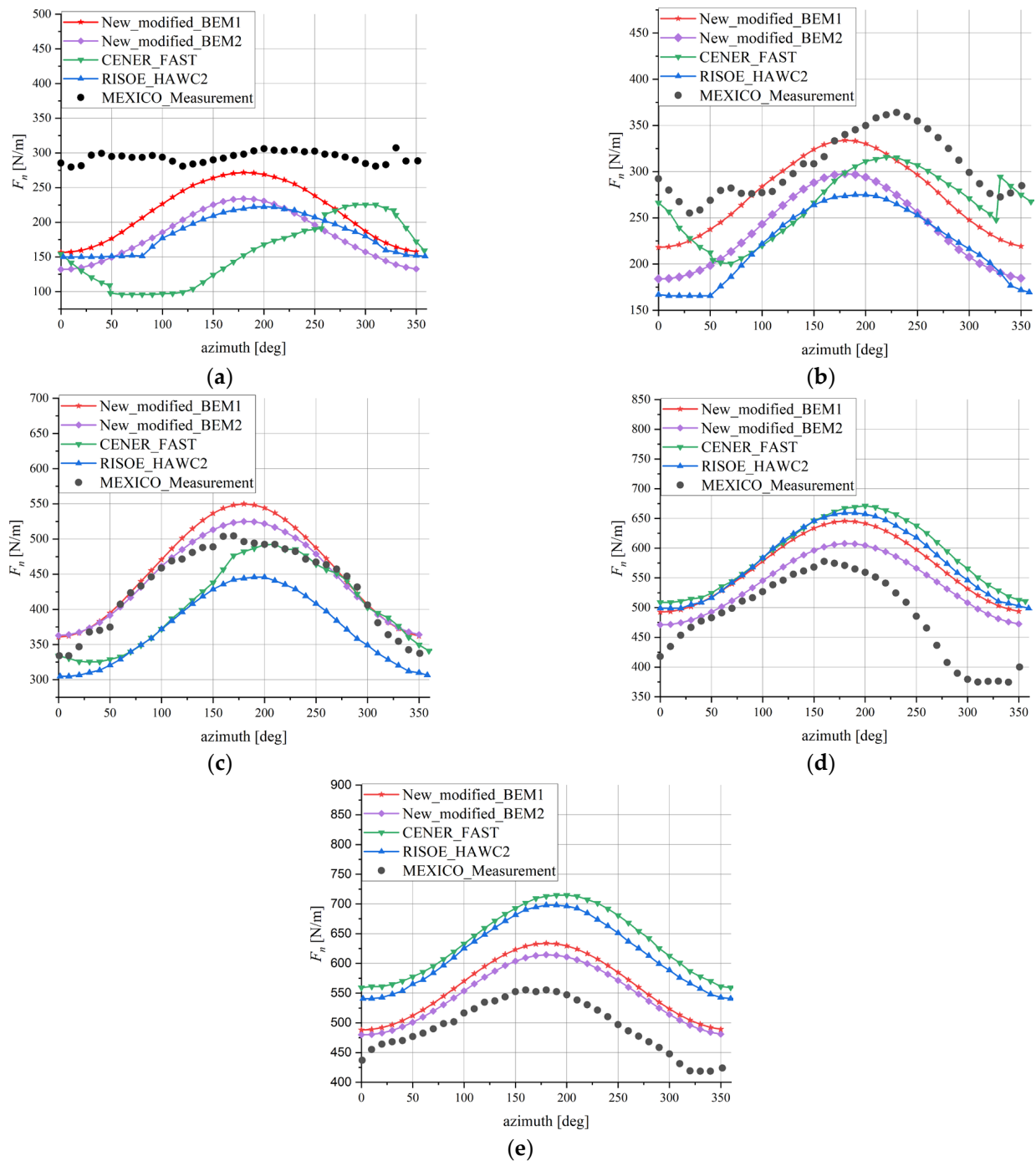


Figure 6. Axial force variation with azimuth angle on the MEXICO rotor at a wind speed of 24 m/s, a yaw angle of 15° and the span station (r/R) of (a) 25%, (b) 35%, (c) 60%, (d) 82%, and (e) 92%.

Figure 7 illustrates the distribution of tangential forces acting on the MEXICO rotor under various azimuth angles when the yaw angle is set to 15° and the wind speed reaches 24 m/s. Due to the occlusion of the icon, the calculated values of CENER FAST and HAWC2 cannot be directly obtained at $r/R = 0.82$ between 70° and 140° , and the calculated values of CENER FAST and HAWC2 between 0° and 140° at $r/R = 0.92$. In order to ensure the beauty of the plot and the integrity of the data, this study adopts the cubic spline interpolation technology to estimate and fill the data points that cannot be directly observed or obtained. In addition, under the specific condition that the r/R ratio is equal to 0.92, in order to improve the interpolation accuracy, this study uses the data cycle characteristics, such as the axial force value at the azimuth angle of 350° is equal to the axial force value at

the azimuth angle of -10° , and so on, and carries out effective data supplement and interpolation processing based on this principle. It should be pointed out that, in view of the interpolation method used to process the data in this study, no quantitative comparative analysis of the error of the tangential force of the model has been carried out. Under this specific combination of wind speed and yaw angle, the experimental data of the tangential forces on the MEXICO rotor do not follow the typical trend of a cosine function but exhibit an irregular pattern, posing a significant challenge for the accurate application of numerical prediction models. At the 25% spanwise position, the results shown in the figure indicate that the calculated values of CENER FAST and HAWC2 are lower than the experimental values, and the CENER FAST model exhibits notable instability. In comparison, the errors of these two models are both higher than those of the new modified model. Moreover, the average value of the new modified BEM1 is close to the experimental average value, and its errors are smaller than that of the new modified BEM2 model at most azimuth angles. At the 35% spanwise position, the error is smaller when the blade rotates to the upper semicircle and larger when it rotates to the lower semicircle. And the accuracy of the new modified BEM1 is greater than that of the new modified BEM2 in this position. As the spanwise position approaches the middle and tip of the blade, the magnitude patterns of the tangential forces predicted by the new modified model and the other two models show similarities to those of axial forces. At $r/R = 0.6$, obviously, although the error of the new modified BEM2 is larger than that of the new modified BEM1, its error is consistently lower than those of CENER FAST and HAWC2 at all azimuth angles, which suggests that the new model possesses a certain degree of accuracy under these conditions. When r/R reaches 0.82, the calculated values of the new modified BEM1 and the other two models are highly similar, while the calculated values of the new modified BEM2 are significantly closer to the experimental values. At $r/R = 0.92$, although the simulated values of the three models are higher than the experimental values, the new modified model's predictions at each azimuth angle are slightly lower than those of the other two models, indicating an improvement in prediction accuracy under these conditions.

In summary, among the models investigated, the new modified model's overall performance exhibits relatively superior predictive accuracy for tangential forces across multiple radial positions and azimuth angle ranges. Particularly in the regions near the blade tip, the errors of BEM2 at various azimuth angles are significantly closer to the experimental values than those of the other models.

In general, the computational outputs of the new modified model exhibit a higher precision when compared to those of CENER FAST and HAWC2 in most critical circumstances. Based on this, it can be deemed that the new modified model possesses the practical feasibility for application.

3.4. Limitations of the New Modified Model

A new modified BEM for calculating the aerodynamic performance of a wind turbine in yaw is employed in this study and two distinct methods were employed to determine the adjustable parameter m within the model. Although the model has demonstrated improved performance in predicting the aerodynamic behaviors of a wind turbine in yaw after enhancements, it is acknowledged that there are limitations that may affect the computational accuracy of the model.

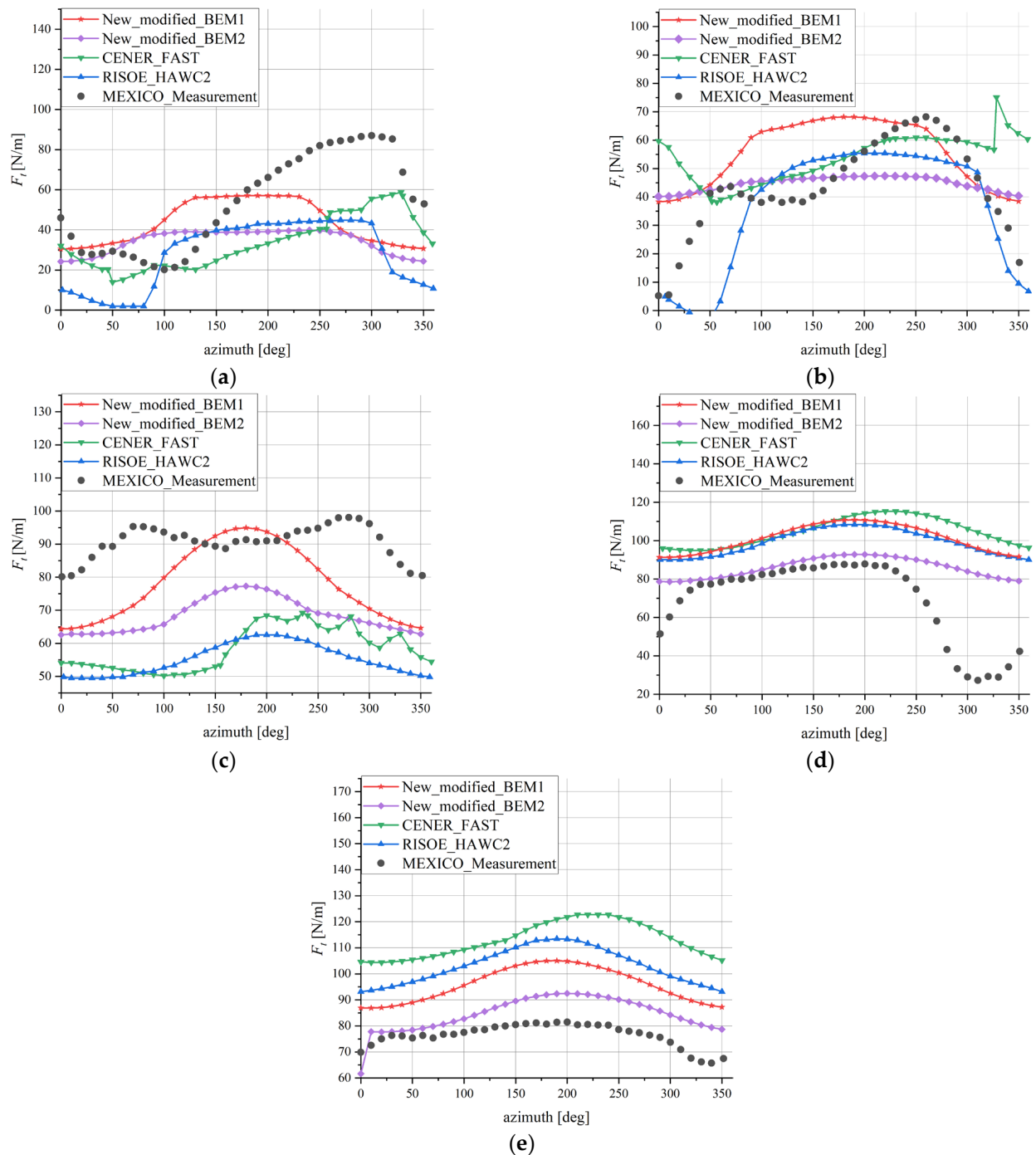


Figure 7. Tangential forces variation with azimuth angle on the MEXICO rotor at a wind speed of 24 m/s, a yaw angle of 30° and the span station (r/R) of (a) 25%, (b) 35%, (c) 60%, (d) 82%, and (e) 92%.

Firstly, while the new modified BEM model introduces a novel momentum theory to mitigate the errors associated with the assumptions of traditional BEM methods, it still assumes that the forces on each blade element are independent of other elements, which might not be entirely accurate under yawed conditions where aerodynamic interactions between the blade elements are likely to be more pronounced. To address this limitation, future research could consider integrating advanced methods, such as the prescribed wake method [33], to more accurately model the aerodynamic coupling between blade elements. Secondly, for the new modified BEM1, the variable factor m is determined based on the 0° yaw condition and is subsequently held constant for predicting blade aerodynamic

characteristics under other yaw angles. However, yaw can alter the aerodynamic conditions, and keeping m constant may introduce some errors. This limitation highlights the need for a more dynamic approach to account for the variability of m under different yaw angles. For the new modified BEM2, the empirical value of m is derived from experimental data. Results indicate that this approach achieves a higher accuracy, particularly in regions away from the blade root. However, the current scarcity of experimental data limits the derivation of a comprehensive empirical formula for m . Only three sets of data are available, which is insufficient for robust observation and fitting. Future research can focus on collecting additional experimental data to derive a reliable empirical formula for m , thereby enhancing the model's predictive capabilities across a broader range of conditions.

Additionally, the results indicate that the advantages of the new model are less pronounced in regions closer to the hub, particularly when compared to regions where the spanwise position is greater than 60%. This may be attributed to the relatively large size of the MEXICO rotor hub. Future research could incorporate hub corrections into the new model to address this limitation. Furthermore, to enhance the applicability of the model to large-scale rotors, additional models such as wind shear and turbulence models could be integrated. These additions would improve the accuracy of the model, making it more suitable for a broader range of applications.

In summary, while the newly modified BEM model demonstrates improvements in predicting the aerodynamic performance of a wind turbine under yaw conditions, several limitations remain. These limitations include the independence assumption of blade element forces, the static treatment of the variable factor m , the scarcity of experimental data for empirical formula derivation, and the less pronounced advantages in regions closer to the hub. Addressing these limitations through advanced aerodynamic coupling methods, dynamic adjustments of parameters, expanded experimental validations, and incorporation of hub and environmental corrections will be crucial for further enhancing the accuracy and applicability of the models. Future research should focus on these areas to develop a more robust and versatile predictive model for wind turbine aerodynamics.

4. Conclusions

Yawed operation is a common and typical condition for horizontal-axis wind turbines. Such yawed conditions subject the blades to increased alternating aerodynamic loads, significantly impacting the service life of the blades. However, the conventional BEM model, due to its assumptions, such as the utilization of a planar disk, introduces relatively large errors when calculating the aerodynamic characteristics of wind turbines under yawed conditions. This paper introduces a new modified BEM method for determining the aerodynamic performance acting on wind turbines under yawed conditions, which initially replaces the momentum theory in traditional BEM with the Madsen analytical linear two-dimensional actuator disc model and integrates the Blade Element Theory with the Madsen model to establish a modified aerodynamic performance prediction model. This substitution circumvents the inaccuracies associated with the planar disc assumption inherent in the momentum theory. Two distinct methods for obtaining the variable parameter m in the new modified model are proposed. The first method combines the new model with a traditional BEM, leveraging the accuracy of the traditional BEM at 0° yaw to determine m for the new model under this condition and then using it to calculate aerodynamic parameters for other yaw angles. The second method directly derives the empirical value of m from experimental data, allowing the new model to use this value directly. Based on the experimental data for the MEXICO rotor, this study conducted a comparative analysis of our newly modified method against existing computational models in CENER FAST and HAWC2. The results indicate that the new modified method provides

a closer alignment with the experimental data in the calculation of aerodynamic forces, particularly in the mid and outer parts. A comparative analysis reveals that the newly modified BEM2 exhibits greater enhancement compared to the newly modified BEM1 and the traditional model. Therefore, this paper recommends using the newly modified BEM2 for predicting aerodynamic performance. At a yaw angle of 30° and a wind speed of 15 m/s, the accuracy is improved by at least 3.5, 1.83, and 3.25 times at the 60%, 82%, and 92% spanwise positions by the new modified BEM2, respectively. Similarly, at a yaw angle of 15° and a wind speed of 24 m/s, the accuracy is enhanced by at least 1.33, 1.67, and 2.6 times at the same spanwise positions. This research endeavors to integrate an emerging momentum theory (Madsen) with the traditional Blade Element Theory, establishing a more precise methodological framework for calculating aerodynamic performance on wind turbines under yaw conditions. A viable research approach for the fusion of a better momentum theory with the blade element theory is offered in this method, thereby contributing a novel perspective to the field of numerical computation of aerodynamic forces on wind turbine blades.

However, the new modified method still exhibits certain limitations that lead to inaccuracies in the aerodynamic force calculations and leave room for future improvements. These limitations include the independence assumption of blade element forces, the static treatment of the variable parameter m , the insufficient experimental data for deriving an empirical formula for m , and the lack of consideration for the hub's influence on aerodynamic forces near the blade root. In light of this, future research should focus on addressing these limitations to develop a more robust and versatile predictive model for wind turbine aerodynamics.

Author Contributions: Conceptualization, J.W. and W.S.; methodology, Z.S., W.Z., C.X. and W.S.; software, J.W., Z.S. and S.F.; validation, W.S.; formal analysis, J.W., Z.S. and W.S.; investigation, J.W. and W.S.; resources, W.S.; data curation, J.W.; writing—original draft preparation, J.W.; writing—review and editing, J.W., C.X. and W.S.; visualization, J.W.; supervision, W.S.; project administration, W.S.; funding acquisition, W.S. and J.W. All authors have read and agreed to the published version of the manuscript.

Funding: This research was funded by 2024 Jiangsu Provincial Carbon Peaking and Carbon Neutrality Science and Technology Innovation Special Project (No. BT2024003) under Jiangsu Province Department of Science and Technology, China, the Key Laboratory on Offshore Wind Energy Research (No. YZ2023247) under Yangzhou Science and Technology Bureau, China, the Postgraduate Research & Practice Innovation Program of Jiangsu Province, China (No. KYCX23_3532).

Data Availability Statement: Data are contained within the article.

Conflicts of Interest: The authors declare no conflicts of interest.

References

1. Wang, X.; Ye, Z.; Kang, S.; Hu, H. Investigations on the Unsteady Aerodynamic Characteristics of a Horizontal-Axis Wind Turbine during Dynamic Yaw Processes. *Energies* **2019**, *12*, 3124. [[CrossRef](#)]
2. Rahimi, H.; Hartvelt, M.; Peinke, J.; Schepers, J.G. Investigation of the current yaw engineering models for simulation of wind turbines in BEM and comparison with CFD and experiment. *J. Phys. Conf. Ser.* **2016**, *753*, 022016. [[CrossRef](#)]
3. Leishman, J.G. Challenges in Modeling the Unsteady Aerodynamics of Wind Turbines. *Wind Energy* **2002**, *5*, 85–132. [[CrossRef](#)]
4. Snel, H.; Schepers, J.G.; Montgomerie, B. The MEXICO project (Model Experiments in Controlled Conditions): The database and first results of data processing and interpretation. *J. Phys. Conf. Ser.* **2007**, *75*, 012014. [[CrossRef](#)]
5. Schepers, J.G.; Snel, H. *Model Experiments in Controlled Conditions*; Technical Report Number ECN-E-07-042; Energy Research Centre of The Netherlands (ECN): Petten, The Netherlands, 2007.
6. Schepers, J.G.; Boorsma, K.; Cho, T.; Gomez-Irardi, S.; Schaffarczyk, P.; Jeromin, A.; Shen, W.Z.; Lutz, T.; Meister, K.; Stoevesandt, B. *Analysis of Mexico Wind Tunnel Measurements: Final Report of IEA Task 29, Mexnext (Phase 1)*; Engineering, Environmental Science; Energy Research Centre of The Netherlands (ECN): Petten, The Netherlands, 2012.

7. Ozbay, A. An experimental investigation on wind turbine aeromechanics and wake interferences among multiple wind turbines. Ph.D. Thesis, Iowa State University, Ames, IA, USA, 2014.
8. Yu, D.O.; Kwon, O.J. Predicting wind turbine blade loads and aeroelastic response using a coupled CFD-CSD method. *Renew. Energy* **2014**, *70*, 183–196. [[CrossRef](#)]
9. Qian, Y.; Zhang, Z.; Wang, T. Comparative Study of the Aerodynamic Performance of the New MEXICO Rotor under Yaw Conditions. *Energies* **2018**, *11*, 833. [[CrossRef](#)]
10. Sorensen, J.N.; Shen, W.Z. Numerical modeling of wind turbine wakes. *J. Fluids Eng.* **2002**, *124*, 393–399. [[CrossRef](#)]
11. Savino, A.; Ferreri, A.; Zanotti, A. Validation of a Mid-Fidelity Numerical Approach for Wind Turbine Aerodynamics Characterization. *Energies* **2024**, *17*, 1517. [[CrossRef](#)]
12. Hansen, M. *Aerodynamics of Wind Turbines*; Earthscan: Routledge, UK, 2008.
13. Lissaman, P.B.S. *Applied Aerodynamics of Wind Power Machines*; Oregon State University: Corvallis, OR, USA, 1974.
14. Burton, T.; Sharpe, D.; Jenkins, N.; Bossanyi, E. *Wind Energy Handbook*; John Wiley and Sons Ltd.: West Sussex, UK, 2001.
15. Gasch, R.; Tvele, J. *Wind Power Plants: Fundamentals, Design, Construction and Operation*; Springer: Berlin/Heidelberg, Germany, 2011.
16. Hansen, M.; Sørensen, J.; Voutsinas, S.; Sørensen, N.; Madsen, H. State of the art in wind turbine aerodynamics and aeroelasticity. *Prog. Aerosp. Sci.* **2006**, *42*, 285–330. [[CrossRef](#)]
17. Hur, C.; Ferreira, C.; Schepers, G. Applicability of Dynamic Inflow Models of HAWT in Yawed Flow Conditions. *Energies* **2022**, *15*, 9368. [[CrossRef](#)]
18. Schepers, J. Engineering models in wind energy aerodynamics. Ph.D. Thesis, Delft University of Technology, Delft, The Netherlands, 2012.
19. Micallef, D. 3D flows near a HAWT rotor: A dissection of blade and wake contributions. Ph.D. Thesis, Delft University of Technology, Delft, The Netherlands, 2012.
20. Liew, J.; Heck, K.S.; Howland, M.F. Unified momentum model for rotor aerodynamics across operating regimes. *Nat. Commun.* **2024**, *15*, 6658. [[CrossRef](#)] [[PubMed](#)]
21. Garrel, A.V. *Development of a Wind Turbine Aerodynamics Simulation Module*; Technical Report Number ECN-C-03-079; Energy Research Centre of The Netherlands (ECN): Petten, The Netherlands, 2003.
22. Jonkman, J.M.; Buhl, M.L. *FAST User's Guide*; National Renewable Energy Laboratory: Golden, CO, USA, 2005.
23. Larsen, T.J.; Hansen, A.M. *How 2 HAWC2, The User's Manual*; Technical Report Number Risø-R-1597; ver. 3-1; Risø National Laboratory: Roskilde, Denmark, 2007; 70p. (In English)
24. Moriarty, P.J.; Hansen, A.C. *AeroDyn Theory Manual*; NREL Technical Report Number TP-500-36881; National Renewable Energy Laboratory: Golden, CO, USA, 2005.
25. Madsen, H.A. An analytical linear two-dimensional actuator disc model and comparisons with computational fluid dynamics (CFD) simulations. *Wind Energy* **2023**, *8*, 1853–1872. [[CrossRef](#)]
26. Shen, W.Z.; Mikkelsen, R.; Sørensen, J.N.; Bak, C. Tip loss corrections for wind turbine computations. *Wind Energy* **2005**, *8*, 457–475. [[CrossRef](#)]
27. Shen, W.Z.; Zhu, W.J.; Sørensen, J.N. Study of tip loss corrections using CFD rotor computations. *J. Phys. Conf. Ser.* **2014**, *555*, 012094. [[CrossRef](#)]
28. Glauert, H. Airplane propellers. In *Aerodynamic Theory*; Durand, W.F., Ed.; Dover: New York, NY, USA, 1963; pp. 169–360.
29. Spera, D.A. *Wind Turbine Technology*; Fairfield: New Jersey, NJ, USA, 1994.
30. Madsen, H.A.; Bak, C.; Døssing, M.; Mikkelsen, R.F.; Øye, S. Validation and modification of the Blade Element Momentum theory based on comparisons with actuator disc simulations. *Wind Energy* **2010**, *13*, 373–389. [[CrossRef](#)]
31. Nocedal, J.; Öztoprak, F.; Waltz, R.A. An interior point method for nonlinear programming with infeasibility detection capabilities. *Optim. Methods Softw.* **2014**, *29*, 837–854. [[CrossRef](#)]
32. Wang, K. A study of cubic spline interpolation. *InSight Rivier Acad. J.* **2013**, *9*, 1–15.
33. Coton, F.N.; Wang, T. The prediction of horizontal axis wind turbine performance in yawed flow using an unsteady prescribed wake model. *Proc. Inst. Mech. Eng. Part A J. Power Energy* **1999**, *213*, 33–43. [[CrossRef](#)]

Disclaimer/Publisher's Note: The statements, opinions and data contained in all publications are solely those of the individual author(s) and contributor(s) and not of MDPI and/or the editor(s). MDPI and/or the editor(s) disclaim responsibility for any injury to people or property resulting from any ideas, methods, instructions or products referred to in the content.